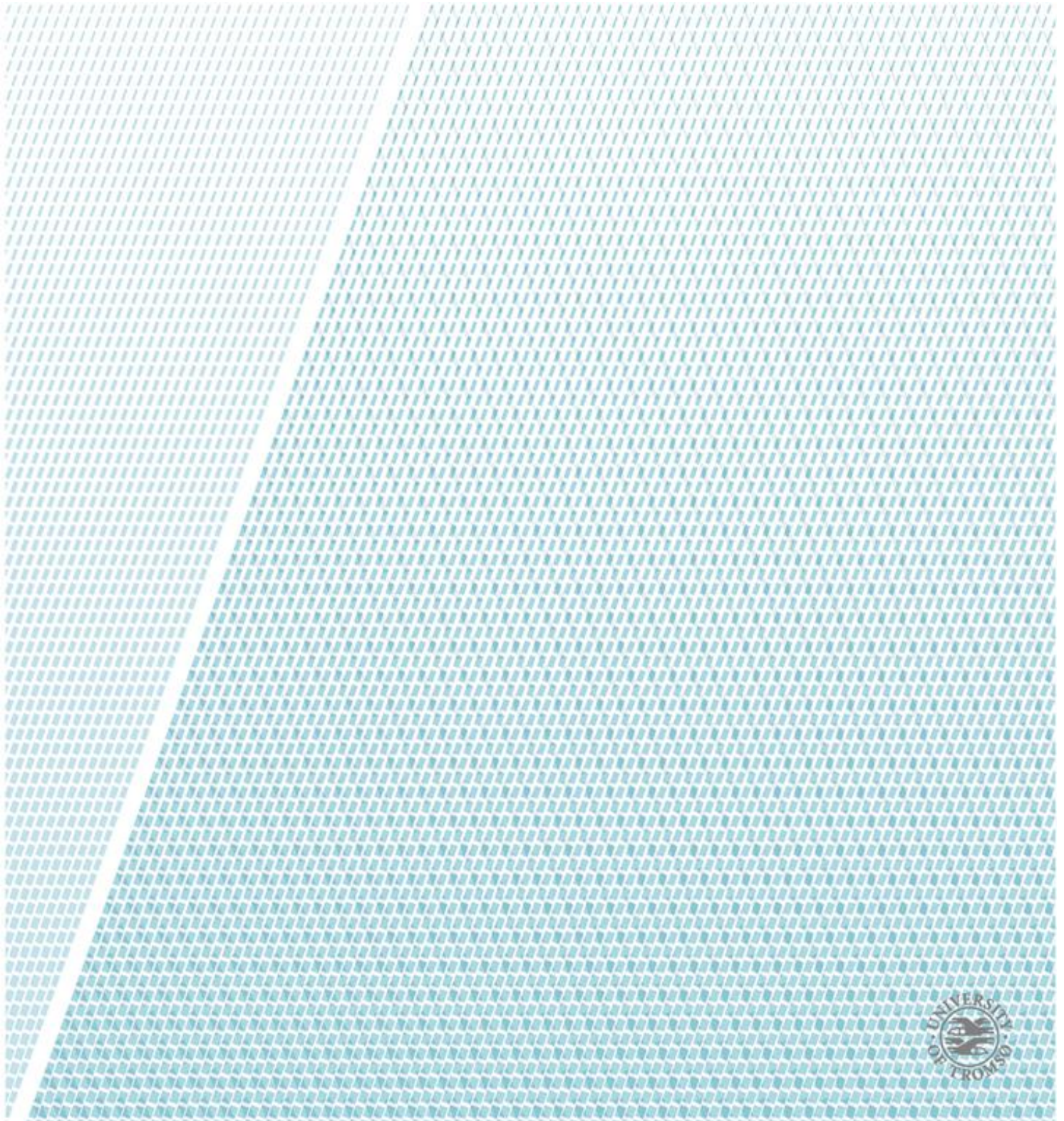Faculty of Health Science

High resolution respirometry in freshly isolated peripheral blood mononuclear cells as a diagnostic method for malignant hyperthermia predisposition
-A pilot study

—

Ahmad Shoeyb Daliri
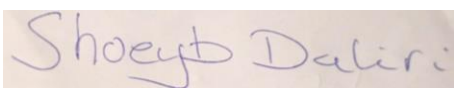*Master thesis in medicine (MED-3950)*

Preface

Writing this thesis has been an amazing journey of both joy and frustration. It has helped me elevate my understanding of knowledge and how it is obtained. There has been moments of joy and moments of despair, but through the entirety of its process I have truly learned to appreciate the hard work done by great minds throughout the world of science.

I want to extend my deepest gratitude to my mentor dr. Mikhail Sovershaev, whom has helped me shape this study. I also want to thank all the great people at the department of biochemical medicine for the extensive help and support I have received.
Without all of you, this paper would not have been a reality.

Last but not least I want to thank my amazing friends and family for their unconditional love and support throughout this time. I will be forever grateful.

Shoeyb Daliri   03.06.2019

I

Table of content

Contents

III

Abstract

Introduction
Malignant hyperthermia (MH) is a potential life-threatening reaction displayed by susceptible patients under general anaesthesia upon encounter with volatile halogenated anaesthetics and succinylcholine.

Background
Biochemically, the development of MH is based upon an abnormal activation of ryanodine receptors in the sarcoplasmic reticulum. Clinically, MH presents with severe signs of hyper catabolism, fever, rigid muscles, respiratory acidosis, metabolic acidosis, tachypnoea, tachycardia, rhabdomyolysis and electrolyte imbalance. The estimated incidence of MH for children and adults undergoing surgery are, respectively, 1:15 000 and 1:50 000 in North American and European populations, although, more recent studies have demonstrated that the incidence of carried MH-trait might be close to 1:2000. To date, diagnostics of MH carrier state still relies on an invasive muscle biopsy *ex vivo* test, warranting the development of a less invasive modality.

Material and method
In this study we have tested whether oxygen consumption by peripheral blood mononuclear cells (PMBCs) exposed to the potent pharmacological opener of Ca channels could be a feasible readout for a diagnostic test for a possible susceptibility of patients to MH development. PBMCs were isolated using standard protocol and oxygen consumption rates were assessed with they use of an oxygraph.
Linear regression was used to assess the rate of oxygen consumption and Wilcoxon signed-rank test was performed to compare the pairwise slopes.

Results
All calculated values using linear regression were significant by a large margin and the R^2 adjusted values was high for all calculated models. Wilcoxon signed-rank test was only significant for three of the 16 pairwise compared experiments and all of them were in discordance with their respective repeated experiments.

Conclusion
This thesis has not provided enough evidence to assume a difference in oxygen consumption rate between PBMCs exposed to the potent RyR activator 4-CMC, and resting PBMCs.

Introduction

Malignant hyperthermia (MH), as first described by doctor Denborough(1), is a potential life-threatening reaction displayed by susceptible patients under general anaesthesia. Upon encounter with certain volatile anaesthetic agents (such as halothane, enflurane, desflurane, isoflurane) or the depolarizing neuromuscular blockade succinylcholine - these patients exhibit severe signs of hyper catabolism, fever, rigid muscles, respiratory acidosis, metabolic acidosis, tachypnoea, tachycardia, rhabdomyolysis and electrolyte imbalance. If not quickly diagnosed and properly treated, tissue damage and or fatality will be the end result(2, 3).

Epidemiology

MH follows an autosomal dominant trait but has an incomplete penetrance with uncertain degree of expressivity. Therefor it is of outmost importance, not only for the patient – but also for their relatives, to diagnose potential genotypes before a surgery induces its phenotype(4). During a five-year period from 2001 to 2005, Brady et al.(5) gathered invaluable data from over 12 million discharged patients across various hospitals in New York. This provided a firm, qualitative understanding of MH susceptibility-risk between genders, with the prevalence being 2.5 – 4.5 times greater in males than females.
For the North-American and European population, the estimated incidence of MH for children and adults undergoing surgery are respectively 1:15 000 and 1:50 000(6, 7). Although, more recent studies have demonstrated that the incidence of carried MH-trait might be close to 1:2000(8).

When first introduced as an anaesthesiologic and genetic condition, the rate of mortality associated with MH was estimated to be around 70-80% (6). However, in the following decades, a significant and drastic reduction in mortality rate occurred. One of the main reasons for the evident abatement in deaths associated with MH was the introduction of dantrolene in 1975 – a pharmacological drug used to revert the pathophysiological effects initiated by triggering agents(9).
H. Ordingen et al.(10) published an article in 1984 that investigated 210 patients with suspected MH. The authors found a mortality rate of 21%, although at this point in time dantrolene had not been used for more than a mere decade. Over the course of the last 40 years, development of capnography, better clinical understanding of the disease and the introduction of effective pharmacological treatment has helped to reduce the mortality rate to 5%(7, 10).

Triggering agents

Volatile anaesthetics such as halothane, isoflurane, sevoflurane, desflurane and enflurane have been mapped as triggering agents for MH. These agents might cause an acute episode of MH alone or in affiliation with succinylcholine, a depolarizing muscle relaxant(11, 12). In the early 90's Louise et al.(13) demonstrated that interaction between volatile anaesthesia and porcine muscles does indeed alter the calcium-release mechanism, in an increasing fashion. This was found to be true even at pH and calcium levels where RyR are expected to remain closed.

Although MH may occur upon first encounter with known triggering agents, patients may also have had exposure prior to the documented case without the onset of an acute MH-episode(14).

Theory and pathophysiology

During a physiological muscle contraction, acetylcholine from neuromuscular endplate gives rise to action potentials which then in turn are propagated in a longitudinal fashion along the muscle fibre. The rapid transition of electrical signals, from the surface of the muscle cells to its interior, is aided by invaginations called transverse tubules (T-Tubules). This mechanism ensures the rapid arrival of action potential namely to the dihydropyridine receptors which in turn undergoes a conformational change and directly transmits the signal to the ryanodine receptors (RyR)(15-17). Calcium is then released from the sarcoplasmic reticulum into the cytosol, resulting in cross-linking of myofilaments and thereby muscle contraction(18, 19).

The importance of well-regulated calcium homeostasis is discernible by the fact that cells maintain a strict level in which calcium operates within. Though calcium concentrations in most cells, especially muscle cells, are maintained at a low level – they can be increased many folds due to internal calcium-storages namely sarcoplasmic/endoplasmic reticulum(20). Another aspect within the basic principles of calcium regulation, which further supports the idea that calcium indeed is of outmost importance to our body, is the fact that extracellular concentration of calcium is 12 000 folds bigger than the intracellular concentration. A substantial amount of energy is dedicated solely for the purpose of maintaining a strict concentration gradient(21).

Patients susceptible to malignant hyperthermia have a genetic mutation causing irregulated flow of calcium from sarcoplasmic reticulum to the intracellular space. This comes as a response to the above-mentioned triggering agents. Although not fully understood, it is believed to be this elevated calcium level which is responsible for the clinical manifestation of the condition as earlier described(22-24).

There are two main receptors in charge of controlling the flow of calcium between intracellular space and sarcoplasmic reticulum– the ryanodine receptors, as mentioned earlier(25), and the inositol 1,4,5-triphosphate receptors (IP3Rs)(26). Three different isoforms of the RyR exists with distinct, although concurrent, functionality. These receptors are termed RyR1 to 3 and are found, in skeletal muscle cells, cardiac cells and smooth muscle cells respectively. Early biomolecular genetic studies recognized ryanodine receptors on chromosome 19 to be the primary locus for malignant hyperthermia susceptibility (MHS)(27). Further genetic studies have established only two genes in which mutations are acknowledged to cause MHS; RyR1(28-31) and calcium voltage-gated channel subunit alpha1 S (CACNA1S)(32).

Clinical manifestations

Establishing a clinical diagnosis of MHS often proves to be difficult. This is partly due to the fact that manifestation of an acute episode, regarding its first signs, can be highly variable. Patients may also present with only a few symptoms, and the symptoms themselves might display varying degree of intensity(33, 34). However, the underlying causes of the rather

fluctuating signs associated with MH are not fully understood. Despite the lack of certain knowledge on this topic, there are a few variables pointed out as possible explanatory causes. These variables are concentration and duration of anaesthesia, age, genetic and temperature(33, 35, 36).

Over the course of almost two decades, from January 1.st 1987 to December 31.st 2006, Larach and colleagues(2) analysed cases of MH reported to the North American Malignant hyperthermia Registry. They found hypercarbia (92,2%) and sinus tachycardia (72,9%) to be among the most common first signs in MH patients. Although not as frequent, master spasm (26,7%) was found to be the earliest sign of MH. Rapidly increasing body temperature (64,7%) and elevated temperature (52,2%) were also frequently displayed by MH patients.

The clinical symptoms associated with MH can be divided into early and late signs. Table 1.0 provides a summary of these signs. It is worth mentioning that increased body temperature indeed is a late sign of MH. From the initiation of an acute MH episode to the clinical manifestation of rise in temperature, often several other symptoms are evident.
Early signs of MH include elevated CO_2 levels, increased O_2 consumption, inappropriate tachycardia, master spasm and generalized muscle rigidity. As for the late signs one can discover increased core body temperature, elevated blood myoglobin levels and disseminated intravascular coagulation(37, 38).

Larach et al.(38) developed a clinical assessment tool developed in 1994 (table 2.0) in order to assist clinical diagnosis. This grading scale is of special importance when time is of essence and MH susceptibility has not been determined prior to surgery. Seven processes have been chosen in the aid of diagnosis, each with an indicator that gives a score based on how strongly the indicator is correlated with MH. The total score is then categorized in six groups ranging from the likelihood being *almost never* to *almost certain* (table 2.1)

Diagnosis of MH
The diagnosis of MH was initially done by clinical observation of the patients. The noticeable symptom exhibited by the condition was an increasing fever which often ended in fatal outcome, hence the name malignant hyperthermia(1, 39, 40). In the 1970's Ellis et al.(41) and Kalow et al.(42) developed an in vitro muscle contracture test with exposure to respectively halothane and caffeine. This development established a dependable source of screening and is still considered the gold standard for MH diagnosis(34, 43). Subsequent standardization trails resulted in the creation of two similar protocols by the European Malignant Hyperthermia Group (EMHG) and the North American Malignant hyperthermia Group (NAMHG)(44). The EMHG and NAMHG named their protocols the in vitro contracture test (IVCT) and the caffeine-halothane contracture test (CHCT), respectively. Even though the IVCT and the CHCT are in many ways similar, a few distinctions do exist between them. For instance the NAMHG allows for the acquirement of a muscle specimen from any muscle site, whereas the protocol developed by the EMHG requires the use of vastus lateralis(45, 46).

In vitro contracture test
As earlier described, assessment of susceptibility to MH is of outmost importance in patients with either prior case of MH or family history with the pharmacogenetic disorder. In 1983

the EMHG(45) established a protocol for in vitro diagnostic of susceptibility to MH which was published a year later. This method challenges muscle specimen from vastus lateralis with caffeine and halothane. The protocol defines three groups based on experimental findings, MH susceptible (MHS), MH negative (MHN) and MH equivocal (MHE). EMHG defines MHS as such: "A caffeine threshold (as defined earlier) at a caffeine concentration of 1.5mmol or less, and a halothane threshold of 2% v/v halothane or less." MHN is defined as:

> A caffeine threshold at a caffeine concentration of 3 mmol or more without a halothane threshold at 3% v/v halothane or less. The term MHN should be reserved to describe a normal patient from a known MH family.

MHE is defined as:

> All other results will be deemed equivocal. The term MHE should be used to describe any patient with an equivocal result, regardless of family background. It is envisaged that some MHE patients will be clinically regarded as MH susceptible. MHE patients must be considered to be under permanent review pending the acquisition of further control data, this being one of the Group's aims.

The caffeine threshold is defined as: "the lowest concentration of caffeine which produces a sustained increase of at least 0.2 g in baseline tension."
Though, as previously mentioned, IVCT is considered to be the golden standard for MH diagnostic, only a few centres around the world performs the analysis. The nearest accredited centre for the Norwegian population is in southern Sweden at the university hospital of Lund(47) and Herlev hospital(48) in Copenhagen, Denmark. Although Institute of Medical Genetics at Ullevål, Oslo is mentioned by the EMHG, they have yet to obtain accredited status.

Scientific problem
Ryanodine receptors are not only expressed in muscle cells but can also be found in a variety of other non-excitable cells, including B and T lymphocytes(49, 50). This provides an excellent basis for exploring alternative diagnostic methods for the susceptibility to MH.

Justification of scientific problem
The in vitro contraction test, used for diagnosing MH, is an extremely invasive method. The incidence of MH might be much higher than previously estimated and since MH is a potentially deadly complication of general anaesthesia(51),development of diagnostic methods for MH susceptibility could potentially reduce number of MH-related deaths further. It is also important from the ethical and professional perspective to establish novel diagnostic tools which do not exclude patient groups such as children and elderly from receiving medical attention. We envision that this thesis will advance us one step further in the direction of the development of minimally invasive diagnostic strategy for testing of susceptibility for MH in all groups of patients in question.

Thesis restrictions
This thesis focuses on testing whether PBMCs are usable cells for diagnostics of MH susceptibility. Given the limited timespan of the present work, we chose only to test the

previously published concentrations of the potent RyR activator, 4-Chloro-m-cresol (4-CMC)(52). Its ability to affect the oxygen consumption of PBMCs was evaluated using high resolution respirometry methodology. Further studies using higher concentrations of 4-CMC are warranted.

Objective

The aim of the study is to evaluate whether there is a difference in oxygen consumption rate between freshly isolated PBMCs exposed to a potent RyR activator and resting PMBCs.

Material and method

In order to assess whether increased intracellular calcium concentration promotes oxygen consumption, PBMCs were challenged with the potent RyR activator (4-CMC)(53). The Oroboros Oxygraph was subsequently used for exact measurement of oxygen concentrations. As described earlier, ryanodine receptors are not exclusive to muscle cells, they can also be found in lymphocytes. Anticoagulated whole blood from the blood bank was used in order to isolate the desired cells.

Equipment, chemicals, and solutions

The department of Biochemical medicine at UNN provided the following machines and solutions:

Machines:

1. Oroboros high resolution respirometry o2k – used to assess oxygen concentrations and their changes in every experiment
2. Centrifuge – used in isolation of PBMC
3. Sysmex XP-300 – used to count PBMC
4. Tube vibrator stirrer – used to obtain homogenous mixtures
5. Haemocytometer – used for assessment of cell viability
6. Microscope – used for assessment of cell viability
7. 50 millilitre tube – used for isolation of PBMCs
8. 5ml pipette – used for isolation of PBMCs
9. 1-1000μl Pipette – used for isolation of PBMCs and trypan blue viability test

Solutions:

1. Phosphate-buffered saline, 0.3% ethylenediaminetetraacetate , 0.1% diethyl pyro carbonate
2. 0.4% trypan blue

All other chemicals and solutions used are bought from the online store of Sigma-Aldrich Oslo, Norway.

1. Lymphoprep^{TM}– density gradient used in isolation of PBMC
2. 4-Chloro-m-Cresol

Isolation of PBMC

Anticoagulated whole blood provided by the blood bank was used in this experimental study. Isolation of PBMCs is widely used and a general protocols exist for careful extraction of these cells(54). The protocol for PBMC isolation is described in detail and was performed as following:

1. 15ml of whole blood was diluted with 15ml of phosphate-buffered saline (PBS), 0.3% ethylenediaminetetraacetate (EDTA), 0.1% diethyl pyro carbonate (DEPC) in a 50 ml tube.
2. 15 ml of Lymphoprep^{TM,} a density gradient, was subsequently added to the bottom of a new 50ml tube. The gradient used has the desired density of 1.077g/ml.
3. Using a 5ml pipette, the PBS-diluted whole blood was carefully extracted and layered on top of the Lymphoprep^{TM}, before performing centrifugation at 2499rpm for 15 minutes without brakes.
4. A 5ml pipette was then used to aspirate the acquired mononuclear cells from centrifugation and were subsequently injected into a new 50ml tube.
5. The 50ml tube was then filled with PBS and centrifuged at 428rpm for 10 minutes with brakes.
6. The supernatant was removed after centrifugation and the 50ml tube containing the mononuclear cells were once again filled with PBS.
7. The cells were then centrifuged at 1360rpm for four minutes. This step was performed twice, making sure that as much platelets as possible were removed.
8. Finally, the supernatant was removed and the obtained PBMCs were diluted with PBS for a total volume of 5ml.
9. The cells were counted using a Sysmex XP-300

The experiments were performed immediately after isolation.

Oxygen consumption measurements

The Oroboros Oxygraph was used to measure the oxygen consumption rate. This device contains a dual chamber configuration, each with a magnetic stirrer to ensure homogenous distribution of the solution. A polarographic oxygen sensor, attached at the floor of each chamber, measures oxygen concentration as an electric current. The measured current is subsequently converted into voltage which in turn is transmitted to a connected computer. The raw signal obtained by the computer is at any given time calibrated to show oxygen concentration in nanomolar per millilitre(55). A superimposed graph shows the time derivative as a negative value. The rationale for this, seemingly mathematical inaccurate decision, is based on basic thermodynamics and physical chemistry explained by Gnaiger(56) in 1993.

The Oroboros Oxygraph calculates the oxygen concentration every 0.5 seconds, and the data is transported in real-time to an attached computer. Oxygen concentration and its time derivative are displayed through Oroboros software, DatLAB. In this software oxygen concentration is presented as an absolute value within a graph where X-axis is defined as time in minutes and Y-axis is defined as oxygen concentration in nanomolar/millilitre. The

superimposed time derivative shares the same X-axis but its Y-axis displays picomolar/ (second x millilitre).

Mitochondrial respiration medium-06

In order to calibrate the oxygen levels, a total volume of 2.0 ml Mitochondrial respiration medium-06 (MIR06) was added to both chambers. Mitochondrial respiration medium was developed in year 2000 and described elsewhere[57]. The medium is formulated[58] primarily for preservation of cells mitochondrial function and oxidative phosphorylation. Although MIR06 does not affect oxygen concentrations directly, it allows for the possibility to increase oxygen levels, if so wanted, without opening the apparatus measurement chamber. This is done by the addition of H_2O_2 which releases O_2[58]. Given the fact that MIR06 does not affect measured oxygen levels, it was chosen as the vehicle for the control group for our cells challenged by 4-CMC. The medium was also used as a vehicle solution for the PBMCs added to both chambers through all the experiments.

Oxygen calibration

Before each experiment, both chambers were calibrated to oxygen concentration in the room. The calibration was performed by not completely sealing off the chambers, and thus letting (i) the oxygen dissolved in MIR06 medium, (ii) the oxygen above MIR06 in the chamber and (iii) the atmospheric oxygen in the room reach steady equilibrium. In order to fully understand this concept, a brief introduction of Henry's law[59] concerning gas solubility is needed. Henry's law states that there is a proportional relationship between the partial pressure of a gas and its solubility in a liquid. The conditions for this rule are constant volume of gas and liquid as well as constant temperatures. Thus, one can conclude that during the oxygen calibration procedure, equilibrium between i, ii and iii would eventually find place. Since our oxygraph measures oxygen concentration and, more importantly, its time derivative, i.e. rate of oxygen concentration changes per unit of time – we could observe in real time when equilibrium was reached. Equilibrium was assumed when the rate of change fluctuated minimally, with values around zero pmol/ (seconds x ml) (figure 1.0). A 10-minute calibration period containing the most stable measurements was then marked and used as the baseline for calibration and further calculations.

Experimental design

After acquiring the desired cells, a total amount of 4.0×10^7 PBMCs were extracted using the basic dilution equation $C_1 \times V_1 = C_2 \times V_2$[60]. The same volume of PBMCs that needed to be added was subtracted from the chambers using a 500µl pipette. This was to ensure that the constant cuvette volume of 2.0ml was maintained. The final concentration of PBMCs in both chambers were always 2.0×10^7 cells/ml.

Given the dual chamber configuration of the Oroboros Oxygraph, each experiment was performed with one chamber having added 4-CMC (intervention) and the other MIR06 (control).Thus, for each round of performed experiments, data was obtained from both the chamber challenged with 4-CMC and the chamber with added MIR06. This provides a better test strategy, eliminating any bias concerning changes in oxygen calibration. Since the whole blood, provided by the blood bank, differed from day to day – we used the same blood on

both conditions. This means that every experiment was performed with the same donor blood in both chambers.

Four different 4-CMC concentrations were used in the experiments, as displayed by table 3.0. Each group of concentration was tested in four independent experiments. To further minimize bias in conjunction with measured oxygen levels, the experiments performed with the intervention and control groups were equally divided between the chambers (also presented in table 3.0).

Table 4.0 provides a representative summary of how every experiment was executed in regard to added volume. A 5-minute time interval was used in between addition of new volumes. This allowed for the repeated measurements of oxygen concentration in response to added 4-CMC or vehicle. Upon oxygen concentration dropping to values between 60nmol/ml – 30nmol/ml, both chambers were re-oxygenated by opening the chambers ever so slightly.

Trypan blue viability test

To make sure that the cells used for the experiment survived the isolation and the experiment itself, we reviewed the state of the cell membranes using the trypan blue viability test, or a so-called Trypan blue exclusion test. This method, which is widely used in the biological studies for assessment of cell viability, is based on the loss of membrane integrity upon cell death. Trypan blue penetration within the cells, provides a quick but also quantitative picture of the survival rate of the cells. The basic idea behind the test is simple. Trypan blue is used to colour the cell followed by examination under microscope. If cell integrity is upheld, the dye will not enter and mix with the cytosol and the cells will not obtain the characteristic blue colour. Thus, if the cell membrane is no longer intact, the cytosol will be stained blue and this will be displayed(61).

A detailed description of the protocol used in this study follows bellow:

1. A total amount of 1.0×10^6 cells were extracted and diluted with PBS for a total volume of 0.5milliliters.
2. 0.4% trypan blue was added in a 1:1 ratio
3. The cells were rested for 5 minutes in room temperature
4. A haemocytometer was used with nine 1x1 mm squares. The four corner squares were used to count the cells.

This was carried out both prior to and after every experiment.

Statistical tests

The rate of oxygen consumption follows a linear decline, as shown in figure 2.0, 2.1, 3.0, 3.1, 4.0, 4.1, 5.0 and 5.1. Therefore, linear regression analysis was performed to obtain the slopes after each volume addition. The use of this model establishes a basis for evaluating whether changes in oxygen consumption differed from chamber A to chamber B, after each successive volume addition. The slopes were compared using the Wilcoxon signed-rank test(62). This test allows for the pairwise comparison of two groups (in this study – intervention and control group) where measurements performed are dependent. There is however no requirement of normal distribution. Since the PBMCs used in our chambers had

successive volume addition, the values obtained must be considered dependent, thus excluding the use of Mann–Whitney U test(63).

For evaluating the trypan blue cell viability, Mann-Whitney U test was performed. The pairwise comparison consists of cell viability prior to experiment in a given chamber, and cell viability after experiment in the same chamber. The rationale for use of this test is that measurements of cell viability were done separately for each experiment and chamber. Therefor all values are considered independent of each other. As with the Wilcoxon signed-rank test, normal distribution is not required.

Results

As demonstrated by figure 2.0, 2.1, 3.0, 3.1, 4.0, 4.1, 5.0 and 5.1 we can observe the oxygen concentration (blue graph) and its time derivative over time (red graph). Although a visible linear decline in oxygen concentration can be monitored in every experiment, it is necessary to evaluate its time derivative as it shows any changes – however small they are. A sudden dip in the time derivative of oxygen concentration occurred immediately upon addition of volumes. This is true for both the intervention and control group. After approximately 1 minute the graphs regained their original slopes, meaning that the oxygen consumption by PBMCs became stable again. It is this slope that is used as a basis for the calculations presented below.

Mann-Whitney U test

Cell viability was assessed by use of trypan blue cell viability test. The results are summarized in tables 5.0 and 5.1. A total average of 98.75% cell viability was calculated for all cells prior to experiments and 98.65% for all cells by the end of the experiments. These results conclude that the vast majority of the cells were alive both prior to and after the experiments. The Mann-Whitney U test showed no significant differences between cell viability before and after experiments (summarized in table 5.2)

Linear regression

Given the fact that all performed experiments in one group were done not only subsequently, but also in the exact same way – four representative tables (tables 6.0,6.1,6.2 and 6.3) are provided as a summary for the linear regression performed. This summary consists of one representative regression analysis from each of the four groups. The alpha level was set to $\alpha=0.05$ and all calculated values were significant by a large margin. R^2 adjusted was used in order to assess the percentage of changes explained by this model. Over 84 percent of the R^2-adjusted values were above 0.500. A significant relation between time and oxygen consumption has been proven. These findings provide substantial evidence that linear regression indeed is an excellent model to evaluate the exact rate of oxygen consumption. Thus, the fundaments for comparison between intervention and control group have been established.

Wilcoxon signed-rank test

The slopes calculated for each volume addition were compared pairwise for every experiment using Wilcoxon signed-rank test. An alpha level of $\alpha=0.05$ was used and the

results are presented in table 7.0. Experiment I in group 1, experiment II in group 4 and experiment IV in group 4 showed statistic significant differences between the chambers. No other experiment, including the three other experiments in group 1 and two other experiments in group 4, showed any significant difference in oxygen consumption rate. The findings demonstrate the importance of repeated measurement in all concentration. Although some of the experiments showed a statistic significant difference, only one experiment demonstrated significantly increased oxygen consumption rate when challenged with 4-CMC.

In summary we can conclude that PBMCs challenged with 4-CMC in concentrations of 25μM, 100μM and 200μM did not provide sufficient evidence for causing changes in oxygen consumption rate. As for the experiments performed with 300μM 4-CMC, our findings were inconclusive regarding the oxygen consumption rates in resting PBMCs and PBMCs challenged with the potent RyR activator. Thus, the conclusion can be made that our study did not provide an overall sufficient level of evidence regarding changes in oxygen consumption rates between PBMCs challenged with 4-CMC and resting PBMCs.

Discussion

Summary of findings

A high average of cell viability of 98.75% before and 98.65% after the experiments was calculated. There were no significant differences between cell viability before and after the experiments.

Quantified rates of oxygen consumption were obtained by using linear regression. This quantification was not only in regard to the experiments as a whole, but for every single volume addition. With all of the measurement being statistic significant, and a high value of R^2 adjusted across the board, one can conclude that the use of linear regression in this experiment was an excellent method of quantifying oxygen consumption rate.

However, only three of the 16 experiment pairs displayed statistic significant differences (exp I group 1, exp II group 4 and exp IV group 4) when we compared the rates.

Interpretation of analysis

For experiment I in group 1 and experiment II in group 4 (table 7.0), mean slope values were found to be more negative in the intervention group than their respective control group. For experiment II in group 4, opposite findings were discovered. Given the fact that the slopes were calculated from the time derivative of oxygen concentrations, a negative slope indicates decreased oxygen consumption rate. This means that out of the three significant findings, two of them had a respective control group with higher oxygen consumption rate. These findings are contradictive of findings in other studies, where 4-CMC leads to increased oxygen consumption(64, 65). However, it is important to bear in mind that these previous studies are performed on swine. As of yet no studies have been published where the relationship between 4-CMC and oxygen consumption, in any type of blood cells, are investigated.

Strengths and limitations

One of the main strengths of this study is the fact that the whole blood used in concurrent experiments were obtained from the same donor. This established genetic equality for both the intervention and control group. In doing so, the risk of having chambers with innate different oxygen consumption rate duo to variation in donor was eliminated. Another strength of this thesis is the simultaneous execution of every paired experiment. As described above, oxygen calibration requires constant air pressure. Therefore, the most ideal way of comparing two groups, when evaluating oxygen consumption, is to have the exact same oxygen calibration for the intervention and control group.

As for limitations of the study, a larger range of concentrations should have been used in order to obtain better knowledge about the effects of 4-CMC. The paper is also limited by the number of experiments performed. Although the experiments were repeated four times for every concentration, additional experiments could have provided important data and further strengthened the outcome.

Conclusion

The experiments performed in this study showed no significant difference in oxygen consumption rate for 13 out of the 16 paired experiments (table 7.0). Out of the three statistically significant findings, two of them were contradictive of previous, well established studies(64, 65) and all of them were in discordance with their respective repeated experiments Thus, the conclusion can be made that this thesis has not provided enough evidence to demonstrate a difference in oxygen consumption rate between freshly isolated PBMCS exposed to a potent RyR activator and resting PBMCs. However, further studies are necessary in order to investigate a larger number of concentrations with several successive repeated measurement of oxygen concentrations and its changes.

Reference

1. M. A. Denborough JFAF, R. R. H. Lovell, P. A. Maplestone, J. D. Vllliers. Anesthetic deaths in a family. Lancet 1960 45.

2. Larach MG, Gronert GA, Allen GC, Brandom BW, Lehman EB. Clinical presentation, treatment, and complications of malignant hyperthermia in North America from 1987 to 2006. Anesth Analg. 2010;110(2):498-507.

3. Denborough M. Malignant hyperthermia. Lancet. 1998;352(9134):1131-6.

4. Maclennan DH, Zvaritch E. Mechanistic models for muscle diseases and disorders originating in the sarcoplasmic reticulum. Biochimica et biophysica acta. 2011;1813(5):948-64.

5. Brady JE, Sun LS, Rosenberg H, Li G. Prevalence of malignant hyperthermia due to anesthesia in New York State, 2001-2005. Anesth Analg. 2009;109(4):1162-6.

6. Britt BA, Kalow W. Malignant hyperthermia: a statistical review. Canadian Anaesthetists' Society journal. 1970;17(4):293-315.

7. Ording H. Incidence of malignant hyperthermia in Denmark. Anesth Analg. 1985;64(7):700-4.

8. Monnier N, Ph.D., Krivosic-Horber R, M.D., Payen J-F, M.D., Ph.D., Kozak-Ribbens G, M.D., Ph.D., Nivoche Y, M.D., Adnet P, M.D., et al. Presence of Two Different Genetic Traits in Malignant Hyperthermia Families: Implication for Genetic Analysis, Diagnosis, and Incidence of Malignant Hyperthermia Susceptibility. Anesthesiology: The Journal of the American Society of Anesthesiologists. 2002;97(5):1067-74.

9. Harrison GG. Control of the malignant hyperpyrexic syndrome in MHS swine by dantrolene sodium. British journal of anaesthesia. 1975;47(1):62-5.

10. Ording H, Ranklev E, Fletcher R. Investigation of malignant hyperthermia in Denmark and Sweden. British journal of anaesthesia. 1984;56(11):1183-90.

11. Rosenberg H, Sambuughin N, Riazi S, Dirksen R. Malignant Hyperthermia Susceptibility. In: Adam MP, Ardinger HH, Pagon RA, Wallace SE, Bean LJH, Stephens K, et al., editors. GeneReviews((R)). Seattle (WA): University of Washington, Seattle. GeneReviews is a registered trademark of the University of Washington, Seattle. All rights reserved.; 1993.

12. Kunst G, Graf BM, Schreiner R, Martin E, Fink RH. Differential effects of sevoflurane, isoflurane, and halothane on Ca2+ release from the sarcoplasmic reticulum of skeletal muscle. Anesthesiology. 1999;91(1):179-86.

13.   Louis CF, Zualkernan K, Roghair T, Mickelson JR. The effects of volatile anesthetics on calcium regulation by malignant hyperthermia-susceptible sarcoplasmic reticulum. Anesthesiology. 1992;77(1):114-25.

14.   Rosenberg H, Davis M, James D, Pollock N, Stowell K. Malignant hyperthermia. Orphanet journal of rare diseases. 2007;2:21.

15.   Gonzalez-Serratos H. Inward spread of activation in vertebrate muscle fibres. The Journal of physiology. 1971;212(3):777-99.

16.   Adrian RH, Costantin LL, Peachey LD. Radial spread of contraction in frog muscle fibres. The Journal of physiology. 1969;204(1):231-57.

17.   Franzini-Armstrong C, Porter KR. SARCOLEMMAL INVAGINATIONS CONSTITUTING THE T SYSTEM IN FISH MUSCLE FIBERS. The Journal of cell biology. 1964;22:675-96.

18.   Smith JS, Imagawa T, Ma J, Fill M, Campbell KP, Coronado R. Purified ryanodine receptor from rabbit skeletal muscle is the calcium-release channel of sarcoplasmic reticulum. The Journal of general physiology. 1988;92(1):1-26.

19.   Lai FA, Erickson HP, Rousseau E, Liu QY, Meissner G. Purification and reconstitution of the calcium release channel from skeletal muscle. Nature. 1988;331(6154):315-9.

20.   CARAFOLI E, MALMSTRÖM K, SIGEL E, CROMPTON M. THE REGULATION OF INTRACELLULAR CALCIUM. Clinical Endocrinology. 1976;5(s1):s49-s59.

21.   Clapham DE. Calcium Signaling. Cell. 2007;131(6):1047-58.

22.   Hirshey Dirksen SJ, Larach MG, Rosenberg H, Brandom BW, Parness J, Lang RS, et al. Special article: Future directions in malignant hyperthermia research and patient care. Anesth Analg. 2011;113(5):1108-19.

23.   Wappler F. Malignant hyperthermia. European journal of anaesthesiology. 2001;18(10):632-52.

24.   Iaizzo PA, Klein W, Lehmann-Horn F. Fura-2 detected myoplasmic calcium and its correlation with contracture force in skeletal muscle from normal and malignant hyperthermia susceptible pigs. Pflugers Archiv : European journal of physiology. 1988;411(6):648-53.

25.   Otsu K, Willard HF, Khanna VK, Zorzato F, Green NM, MacLennan DH. Molecular cloning of cDNA encoding the Ca^{2+} release channel (ryanodine receptor) of rabbit cardiac muscle sarcoplasmic reticulum. The Journal of biological chemistry. 1990;265(23):13472-83.

26.   Nixon GF, Mignery GA, Somlyo AV. Immunogold localization of inositol 1,4,5-trisphosphate receptors and characterization of ultrastructural features of the sarcoplasmic reticulum in phasic and tonic smooth muscle. Journal of muscle research and cell motility. 1994;15(6):682-700.

27.   Chen SRW, Vaughan DM, Airey JA, Coronado R, MacLennan DH. Functional expression of cDNA encoding the calcium release channel (ryanodine receptor) of rabbit skeletal muscle sarcoplasmic reticulum in COS-1 cells. Biochemistry. 1993;32(14):3743-53.

28.   Sambuughin N, Holley H, Muldoon S, Brandom BW, de Bantel AM, Tobin JR, et al. Screening of the entire ryanodine receptor type 1 coding region for sequence variants associated with malignant hyperthermia susceptibility in the north american population. Anesthesiology. 2005;102(3):515-21.

29.   Galli L, Orrico A, Lorenzini S, Censini S, Falciani M, Covacci A, et al. Frequency and localization of mutations in the 106 exons of the RYR1 gene in 50 individuals with malignant hyperthermia. Human mutation. 2006;27(8):830.

30.   Robinson R, Carpenter D, Shaw MA, Halsall J, Hopkins P. Mutations in RYR1 in malignant hyperthermia and central core disease. Human mutation. 2006;27(10):977-89.

31.   Kraeva N, Riazi S, Loke J, Frodis W, Crossan ML, Nolan K, et al. Ryanodine receptor type 1 gene mutations found in the Canadian malignant hyperthermia population. Canadian journal of anaesthesia = Journal canadien d'anesthesie. 2011;58(6):504-13.

32.   Stewart SL, Hogan K, Rosenberg H, Fletcher JE. Identification of the Arg1086His mutation in the alpha subunit of the voltage-dependent calcium channel (CACNA1S) in a North American family with malignant hyperthermia. Clinical genetics. 2001;59(3):178-84.

33.   Hopkins PM. Malignant hyperthermia: advances in clinical management and diagnosis. British journal of anaesthesia. 2000;85(1):118-28.

34.   Litman RS, Rosenberg H. Malignant hyperthermia: update on susceptibility testing. Jama. 2005;293(23):2918-24.

35.   Levitt RC, Nouri N, Jedlicka AE, McKusick VA, Marks AR, Shutack JG, et al. Evidence for genetic heterogeneity in malignant hyperthermia susceptibility. Genomics. 1991;11(3):543-7.

36.   Iaizzo PA, Kehler CH, Carr RJ, Sessler DI, Belani KG. Prior hypothermia attenuates malignant hyperthermia in susceptible swine. Anesth Analg. 1996;82(4):803-9.

37.   Glahn KP, Ellis FR, Halsall PJ, Muller CR, Snoeck MM, Urwyler A, et al. Recognizing and managing a malignant hyperthermia crisis: guidelines from the European Malignant Hyperthermia Group. British journal of anaesthesia. 2010;105(4):417-20.

38.   Larach MG, Localio AR, Allen GC, Denborough MA, Ellis FR, Gronert GA, et al. A clinical grading scale to predict malignant hyperthermia susceptibility. Anesthesiology. 1994;80(4):771-9.

39.   Cullen WG. Malignant hyperpyrexia during general anaesthesia: A report of two cases. Canadian Anaesthetists' Society Journal. 1966;13(5):437-43.

40.   Britt BA, Gordon RA. Three cases of malignant hyperthermia with special consideration of management. Canadian Anaesthetists' Society Journal. 1969;16(2):99.

41.   Ellis FR, Harriman DG, Keaney NP, Kyei-Mensah K, Tyrrell JH. Halothane-induced muscle contracture as a cause of hyperpyrexia. British journal of anaesthesia. 1971;43(7):721-2.

42.   Kalow W, Britt BA, Terreau ME, Haist C. Metabolic error of muscle metabolism after recovery from malignant hyperthermia. Lancet. 1970;2(7679):895-8.

43.   EUROPEAN MALIGNANT HYPERPYREXIA GROUP. British journal of anaesthesia. 1984;56(11):1181-2.

44.   Kim D-C. Malignant hyperthermia. Korean J Anesthesiol. 2012;63(5):391-401.

45.   A protocol for the investigation of malignant hyperpyrexia (MH) susceptibility. The European Malignant Hyperpyrexia Group. British journal of anaesthesia. 1984;56(11):1267-9.

46.   Larach MG. Standardization of the caffeine halothane muscle contracture test. North American Malignant Hyperthermia Group. Anesth Analg. 1989;69(4):511-5.

47.   EMHG. Lund [Accredited labs]. Copenhagen: EMHG; 2018 [updated January 7.th 2018; cited 2019 30.05]. Available from: https://www.emhg.org/mh-units/2018/1/7/lund.

48.   EMHG. Copenhagen [Accredited labs]. Herlev, Denmark: EMHG; 2018 [updated January 7.th 2018; cited 2019 30.05]. Available from: https://www.emhg.org/mh-units/2018/1/7/copenhagen.

49.   Hosoi E, Nishizaki C, Gallagher KL, Wyre HW, Matsuo Y, Sei Y. Expression of the Ryanodine Receptor Isoforms in Immune Cells. The Journal of Immunology. 2001;167(9):4887-94.

50.   Sei Y, Gallagher KL, Basile AS. Skeletal muscle type ryanodine receptor is involved in calcium signaling in human B lymphocytes. The Journal of biological chemistry. 1999;274(9):5995-6002.

51.   Larach MG, Brandom BW, Allen GC, Gronert GA, Lehman EB. Malignant hyperthermia deaths related to inadequate temperature monitoring, 2007-2012: a report from the North American malignant hyperthermia registry of the malignant hyperthermia association of the United States. Anesth Analg. 2014;119(6):1359-66.

52.   Hoppe K, Hack G, Lehmann-Horn F, Jurkat-Rott K, Wearing S, Zullo A, et al. Hypermetabolism in B-lymphocytes from malignant hyperthermia susceptible individuals. Sci Rep. 2016;6:33372-.

53.   Herrmann-Frank A, Richter M, Sarközi S, Mohr U, Lehmann-Horn F. 4-chloro-m-cresol, a potent and specific activator of the skeletal muscle ryanodine receptor. Biochimica et Biophysica Acta (BBA) - General Subjects. 1996;1289(1):31-40.

54.   Kleiveland CR. Peripheral Blood Mononuclear Cells. In: Verhoeckx K, Cotter P, López-Expósito I, Kleiveland C, Lea T, Mackie A, et al., editors. The Impact of Food Bioactives on Health: in vitro and ex vivo models. Cham: Springer International Publishing; 2015. p. 161-7.

55.   E. G. Mitochondrial pathways and respiratory control. An introduction to OXPHOS analysis. 3rd ed. Innsbruck: Mitochondr Physiol Network 17.18. Oroboros MiPNet Publications; 2012.

56.   Gnaiger E. Nonequilibrium thermodynamics of energy transformations1993. 1983-2002 p.

57.   Gnaiger E, V. Kuznetsov A, Schneeberger S, Seiler R, Brandacher G, Steurer W, et al. Mitochondria in the Cold. 2000. p. 431-42.

58.   M F, M F-A, E G. Mitochondrial respiration medium - MiR06. Mitochondr Physiol Network. 2016;14.13(06):1-4.

59.   Henry W, Banks J. III. Experiments on the quantity of gases absorbed by water, at different temperatures, and under different pressures. Philosophical Transactions of the Royal Society of London. 1803;93:29-274.

60.   Gucker FT. The Apparent Molal Expansibility of Electrolytes and the Coefficient of Expansibility (Thermal Expansion) as a Function of Concentration1. Journal of the American Chemical Society. 1934;56(5):1017-21.

61.   Strober W. Trypan Blue Exclusion Test of Cell Viability. Current Protocols in Immunology. 1997;21(1):A.3B.1-A.3B.2.

62.   Wilcoxon F. Individual Comparisons by Ranking Methods. Biometrics Bulletin. 1945;1(6):80-3.

63.   Mann HB, Whitney DR. On a Test of Whether one of Two Random Variables is Stochastically Larger than the Other. Ann Math Statist. 1947;18(1):50-60.

64.   Wappler F, MD, Scholz J, MD, Fiege M, MD, Kolodzie K, MS, Kudlik C, MS, Weibhorn R, MD, et al. 4-Chloro-m-cresol is a Trigger of Malignant Hyperthermia in Susceptible Swine. Anesthesiology: The Journal of the American Society of Anesthesiologists. 1999;90(6):1733-40.

65.   Galloway GJ, Denborough MA. Suxamethonium chloride and malignant hyperpyrexia. British journal of anaesthesia. 1986;58(4):447-50.

Tables

Table 1.0 Clinical signs of MH		
Clinical signs		
Early signs	Metabolic	Inappropriately elevated CO_2 production (raised end-tidal CO_2 on capnography, tachypnoea if breathing spontaneously).
		Increased O_2 consumption.
		Mixed metabolic and respiratory acidosis.
		Profuse sweating.
		Mottling of skin.
	Cardiovascular	Inappropriate tachycardia.
		Cardiac arrhythmias (especially ectopic ventricular beats and ventricular bigeminy).
		Unstable arterial pressure.
	Muscle	Masseter spasm if succinylcholine has been used.
		Generalized muscle rigidity.
Late signs		Hyperkaliemia.
		Rapid increase in core body temperature.
		Grossly elevated blood creatine phosphokinase levels.
		Grossly elevated blood myoglobin levels.
		Dark-colored urine due to myoglobinuria.
		Severe cardiac arrhythmias and cardiac arrest.
		Disseminated intravascular coagulation.
This table was created by Glahn et al. (37) as part of the European Malignant Hyperpyrexia Group's guidelines in October 2010.		
This table provides a clinical summary for the signs associated with MH. The signs are divided into *early* and *late* in conjunction with moment of observation.		

Table 2.0 Clinical grading scale		
Process	**Indicator**	**Points**
Process 1 rigidity	Generalized muscular rigidity (in absence of shivering due to hypothermia, or during or immediately following emergence from inhalational general anesthesia	15
	Masseter spasm shortly following succinylcholine administration	15
Process II: Muscle breakdown	Elevated creatinine kinase >20 000 IU after anesthetic that include succinylcholine	15
	Elevated creatine kinase >10,000 IU after anesthetic without succinylcholine	15
	Cola colored urine in perioperative period	10
	Myoglobin in urine >60g/L	10
	Myoglobin in serum>170µg/L	5
	Blood/plasma/serum K+ > 6 mEq/L (in absence of renal failure)	3
Process III: Respiratory acidosis	PET_{CO_2}>55 mmHg with appropriately controlled ventilation	15
	Arterial Pa_{CO_2}>60 mmHg with appropriately controlled ventilation	15
	PET_{CO_2} >60 mmHg with spontaneous ventilation	15
	Arterial Pa_{CO_2}>65 mmHg with spontaneous ventilation	15
	Inappropriate hypercarbia (in anesthesiologist's judgment)	15
	Inappropriate tachypnea	10
Process IV: Temperature increase	Inappropriately rapid increase in temperature (in anesthesiologist's judgment)	15
	Inappropriately increased temperature > 38.8°C (101.8*F) in the perioperative period (in anesthesiologist's judgment)	10
Process V: Cardiac involvement	Inappropriate sinus tachycardia	3
	Ventricular tachycardia or ventricular fibrillation	3

Process VI: Family history (used to determine MH susceptibility only)	Positive MH family history in relative of first degree*	15
	Positive MH family history in relative not of first degree*	5
Other indicators that are not part of a single process **	Arterial base excess more negative than −8 mEq/L	10
	Arterial pH <7.25	10
	Rapid reversal of MH signs of metabolic and/or respiratory acidosis with iv dantrolene	5
	Positive MH family history together with another indicator from the patient's own anesthetic experience other than elevated resting serum creatine kinase *	10
	Resting elevated creatine kinase * (In patient with a family history of MH)	10

* These indicators should only be used for determining MH susceptibility
** These should be added without regard to double-counting

This table was created by Larach, M. G. et al. "A clinical grading scale to predict malignant hyperthermia susceptibility" (38).

Using this grading scale, one can calculate the likelihood of a patient having an acute MH episode. The scores are matched to a rank which in turn is matched to a description of likelihood.

Table 2.1 Clinical grading scale – interpretation		
Raw score range	**MH rank**	**Description of likelihood**
0	1	Almost never
3 – 9	2	Unlikely
10 – 19	3	Somewhat less likely
20 – 34	4	Somewhat greater than likely
35 – 49	5	Very likely
>50	6	Almost certain

This table was created by Larach, M. G. et al. "A clinical grading scale to predict malignant hyperthermia susceptibility"(38)

The total score obtained in table 2.1 is associated with a MH rank as described in this table. The higher the rank, the higher the possibility of an MH episode.

Table 3.0 Performing the experiments			
Group	Experiment	Substance added to chamber A	Substance added to chamber B
1	I	25µM 4-CMC	MiR06
	II	MiR06	25µM 4-CMC
	III	25µM 4-CMC	MiR06
	IV	MiR06	25µM 4-CMC
2	I	100µM 4-CMC	MiR06
	II	MiR06	100µM 4-CMC
	III	100µM 4-CMC	MiR06
	IV	MiR06	100µM 4-CMC
3	I	200µM 4-CMC	MiR06
	II	MiR06	200µM 4-CMC
	III	200µM 4-CMC	MiR06
	IV	MiR06	200µM 4-CMC
4	I	300µM 4-CMC	MiR06
	II	MiR06	300µM 4-CMC
	III	300µM 4-CMC	MiR06
	IV	MiR06	300µM 4-CMC

The experiments were divided into four groups, each containing a different concentration of 4-CMC. Every group contains four repeated experiments (I-IV). The table also provides information about what substances were added to the different chambers in the different experiments

Table 4.0 Addition of volumes		
Time of added volume	Volume of added 4-CMC	Volume of added MIR06
0 minute	5µl	5µl
5 minutes	5 µl	5µl
10 minutes	10 µl	10µl
15 minutes	10 µl	10 µl
20 minutes	15 µl	15 µl
25 minutes	15 µl	15 µl
30 minutes	20 µl	20 µl
35 minutes	20 µl	20 µl

A 5-minute interval was used when adding substances to the chambers. This table provides information about the timeframe between addition of substances.
Note that this table does not account for the time the chambers were open for re-oxygenation. Thus, the total times used in performing the different experiments vary.

Table 5.0 Cell viability using trypan blue test Before experiment								
	Group 1		**Group 2**		**Group 3**		**Group 4**	
Experiment	25µM 4-CMC	MIR06	100µM 4-CMC	MIR06	200µM 4-CMC	MIR06	300µM 4-CMC	MIR06
I	98%	98%	99%	100%	100%	99%	99%	98%
II	99%	98%	99%	99%	100%	97%	98%	99%
III	99%	99%	99%	99%	98%	100%	99%	98%
IV	97%	98%	100%	98%	98%	100%	99%	99%
Total sum of all experiments								3160
N								32
Total average								98.75

The percentage of living cells defined as cells intact membrane before the start of experiment I-IV in the different groups. Tryptan blue colouring was used to determine whether cell membrane integrity was upheld.

Table 5.1 Cell viability using trypan blue test After experiment								
	Group 1		**Group 2**		**Group 3**		**Group 4**	
Experiment	25µM 4-CMC	MIR06	100µM 4-CMC	MIR06	200µM 4-CMC	MIR06	300µM 4-CMC	MIR06
I	98%	98%	100%	98%	100%	99%	99%	98%
II	98%	98%	99%	99%	100%	99%	98%	99%
III	99%	99%	100%	99%	99%	98%	98%	98%
IV	97%	98%	99%	99%	99%	99%	98%	98%
Total sum of all experiments								3157
N								32
Total average								98.65

The percentage of living cells defined as cells having intact membrane after experiment I-IV. Tryptan blue colouring was used to determine whether cell membrane integrity was upheld.

Table 5.2 Mann-Whitney U test for trypan blue cell viability before and after experiment								
Experiment	P-value							
	25µM 4-CMC	MIR06	100µM 4-CMC	MIR06	200µM 4-CMC	MIR06	300µM 4-CMC	MIR06
I-IV	0.486	1.000	0.686	0.686	0.686	0.486	0.343	0.686

Alpha level of 0.05. No significant differences were found between the groups using the Mann-Whitney U Test

Table 6.0 Regression analysis of group 1 – Experiment I

Experiment 25µM 4-CMC vs MIR06

Volume addition	Regression analysis of 4-CMC			Regression analysis of MIR06		
	Coefficient	R^2 adjusted	Significance F	Coefficient	R^2 adjusted	Significance F
5µl	-0.115	0.986	0.000	-0.029	0.791	0.000
5 µl	-0.036	0.959	0.000	-0.0901	0.944	0.000
10 µl	-0.063	0.961	0.000	-0.006	0.328	0.000
10 µl	-0.041	0.315	0.000	-0.026	0.838	0.000
15 µl	-0.114	0.993	0.000	-0.018	0.507	0.000
15 µl	-0.233	0.995	0.000	-0.208	0.984	0.000
20 µl	-0.089	0.949	0.000	-0.059	0.828	0.000
20 µl	-0.113	0.987	0.000	-0.007	0.896	0.000

Alpha level of 0.05. Summary of the regression analysis performed on group 1, experiment 1. The coefficient is the rate of slope obtained from the time derivative. R^2adjusted is the description of how well the linear graph obtained by the regression model describes the changes. F-values of 0.05 or lower are considered significant.

Table 6.1 Regression analysis of group 2 – Experiment I

Experiment 100µM 4-CMC vs MIR06

Volume addition	Regression analysis of 4-CMC			Regression analysis of MIR06		
	Coefficients	R^2 adjusted	Significance F	Coefficients	R^2 adjusted	Significance F
5µl	-0.008	0.848	0.000	-0.053	0.675	0.000
5 µl	-0.176	0.965	0.000	-0.046	0.931	0.000
10 µl	-0.031	0.929	0.000	-0.033	0.749	0.000
10 µl	-0.002	0.765	0.000	-0.047	0.843	0.000
15 µl	-0.039	0.639	0.000	-0.036	0.410	0.000
15 µl	-0.009	0.114	0.035	-0.017	0.414	0.000
20 µl	0.024	0.810	0.000	-0.008	0.223	0.004
20 µl	-0.020	0.842	0.000	0.005	0.423	0.000

Alpha level of 0.05. Summary of the regression analysis performed on group 2, experiment 1. The coefficient is the rate of slope obtained from the time derivative. R^2adjusted is the description of how well the linear graph obtained by the regression model describes the changes. F-values of 0.05 or lower are considered significant.

Table 6.2 Regression analysis of group 3 – Experiment I

Experiment 200µM 4-CMC vs MIR06

Volume addition	Regression analysis of 4-CMC			Regression analysis of MIR06		
	Coefficients	R^2 adjusted	Significance F	Coefficients	R^2 adjusted	Significance F
5µl	-0.035	0.586	0.000	-0.084	0.592	0.000
5 µl	0.061	0.874	0.000	0.117	0.95	0.000
10 µl	-0.044	0.804	0.000	-0.089	0.897	0.000

10 µl	0.008	0.263	0.001	-0.033	0.511	0.000
15 µl	0.067	0.670	0.000	-0.080	0.937	0.000
15 µl	-0.041	0.773	0.00	-0.070	0.777	0.000
20 µl	0.040	0.898	0.000	0.050	0.889	0.000
20 µl	-0.019	0.91	0.000	-0.039	0.851	0.000

Alpha level of 0.05. Summary of the regression analysis performed on group 3, experiment 1. The coefficient is the rate of slope obtained from the time derivative. R^2adjusted is the description of how well the linear graph obtained by the regression model describes the changes. F-values of 0.05 or lower are considered significant.

Table 6.3 Regression analysis of group 4 – Experiment I

Table x

Experiment 300µM 4-CMC vs MIR06

Volume addition	Regression analysis of 4-CMC			Regression analysis of MIR06		
	Coefficients	R^2 adjusted	Significance F	Coefficients	R^2 adjusted	Significance F
5µl	-0.123	0.981	0.000	-0.097	0.927	0.000
5 µl	-0.170	0.983	0.000	-0.049	0.963	0.000
10 µl	-0.055	0.984	0.000	-0.047	0.958	0.000
10 µl	-0.054	0.929	0.000	0.004	0.518	0.000
15 µl	-0.054	0.942	0.000	-0.027	0.332	0.000
15 µl	-0.025	0.750	0.000	-0.063	0.919	0.000
20 µl	-0.0178	0.806	0.000	-0.019	0.490	0.000
20 µl	-0.132	0.994	0.000	-0.1501	0.966	0.000

Alpha level of 0.05. Summary of the regression analysis performed on group 4, experiment 1. The coefficient is the rate of slope obtained from the time derivative. R^2adjusted is the description of how well the linear graph obtained by the regression model describes the changes. F-values of 0.05 or lower are considered significant.

Table 7.0 Wilcoxon signed-rank test for all groups and experiments

Group	Exp		N	Mean	Std. Deviation	Min slope value	Max slope value	P-value
1	I	MIR	8	-.0623	.06482	-.21	-.01	0.050
		CMC	8	-.1011	.06245	-.23	-.04	
	II	MIR	8	-.0553	.07211	-.13	.08	0.208
		CMC	8	-.0171	.04288	-.07	.04	
	III	MIR	8	.4798	1.56426	-.20	4.35	0.123
		CMC	8	.5532	1.71384	-.16	4.79	
	IV	MIR	8	.1110	.45886	-.09	1.24	0.575
		CMC	8	.0843	.50957	-.14	1.34	
2	I	CMC	8	-.0297	.02081	-.05	.01	0.575
		MIR	8	-.0330	.06109	-.18	.02	

				Mean	Std	Lower	Upper	p-value
	II	**MIR**	8	-.0373	.05320	-.11	.03	0.889
		CMC	8	-.0350	.05023	-.12	.02	
	III	**MIR**	8	-.0287	.02903	-.06	.02	0.889
		CMC	8	-.0256	.06052	-.08	.07	
	IV	**CMC**	8	-.0340	.06951	-.14	.05	0.779
		MIR	8	-.0226	.04878	-.10	.04	
3	I	**MIR**	8	-.0288	.07457	-.09	.12	0.161
		CMC	8	.0045	.04662	-.04	.07	
	II	**MIR**	8	-.0350	.05023	-.12	.02	0.093
		CMC	8	-.0658	.05117	-.14	.02	
	III	**MIR**	8	-.1005	.05077	-.19	-.05	0.263
		CMC	8	-.0690	.03280	-.11	-.01	
	IV	**MIR**	8	-.0396	.06983	-.16	.07	0.674
		CMC	8	-.0548	.05322	-.17	-.01	
4	I	**MIR**	8	-.0563	.04859	-.15	.00	0.263
		CMC	8	-.0793	.05539	-.17	-.02	
	II	**MIR**	8	-.0031	.04560	-.09	.05	0.017
		CMC	8	-.1461	.21910	-.66	.04	
	III	**MIR**	8	.0098	.06086	-.05	.13	0.575
		CMC	8	-.0080	.06742	-.10	.09	
	IV	**MIR**	8	-.0516	.04788	-.10	.02	0.05
		CMC	8	-.0199	.06359	-.13	.07	

A summary of the Wilcoxon signed-rank test. Alpha level of 0.05. Mean is a description of the average value of the slopes in that chamber.
P-values of 0.05 or lower were considered significant.

Figures

Figure 1.0 Oxygen calibration
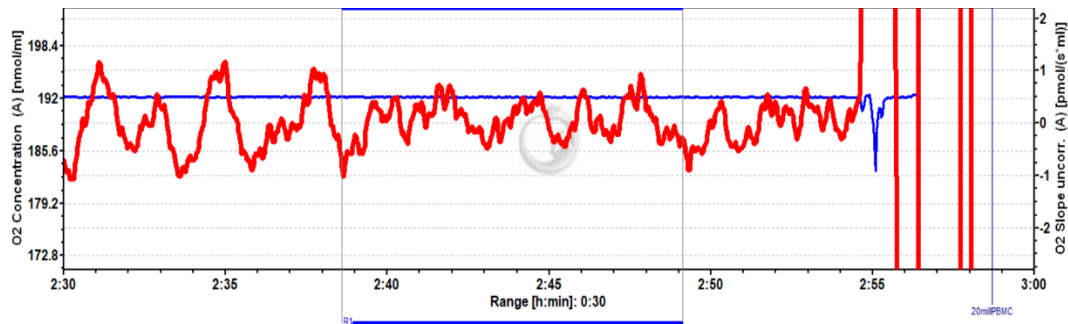
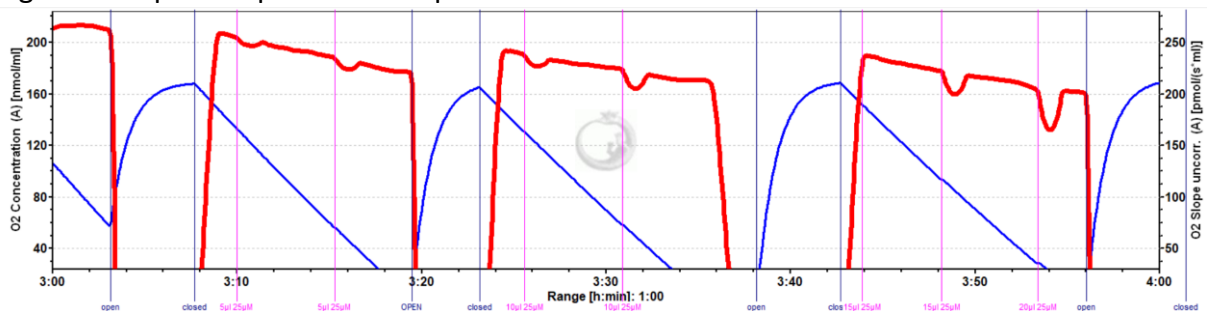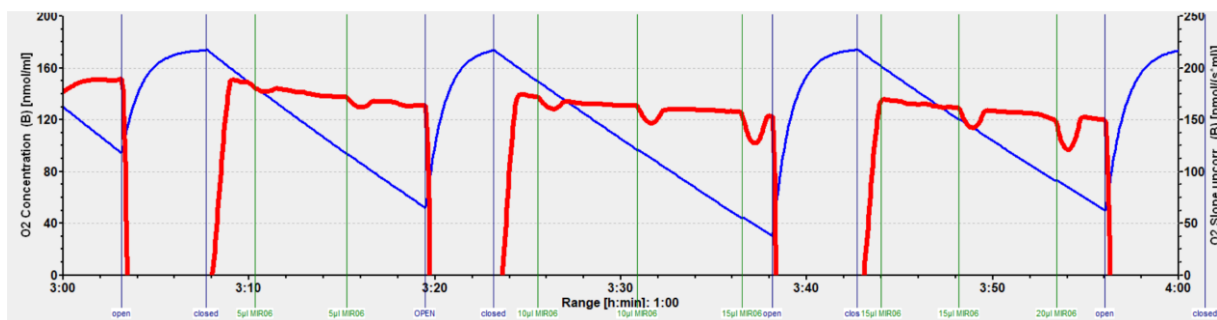Figure 1. A representative demonstration of oxygen calibration. The blue graph shows continuously measured oxygen concentrations presented (Y-axis to the left, nmol/ml). The red graph shows the time derivative of the oxygen concentrations (Y-axis to the right, as pmol/ (seconds x ml)). The displayed values of the red graph, within the marked area (square), is between -1 to +1. Since the red graph is the time derivative of oxygen concentration, fundamental mathematical differentiation indicated that there are no changes in oxygen concentration as the values displayed on the blue graph, demonstrate the level of 192 nmol/ml throughout the stabilization baseline period.

Fig 2.0 Group 1 – 25µM 4-CMC experiment I

Figure 2.0. The blue graph shows continuously measured oxygen concentrations presented (Y-axis to the left, nmol/ml). The red graph shows the time derivative of the oxygen concentrations (Y-axis to the right, as pmol/ (seconds x ml)). This graph displays how oxygen concentration changes in response to addition of 25µM 4-CMC. The time derivative of oxygen consumption is superimposed and displayed as the red graph. Notice the slight dip in the red graph after each successive addition of 4-CMC
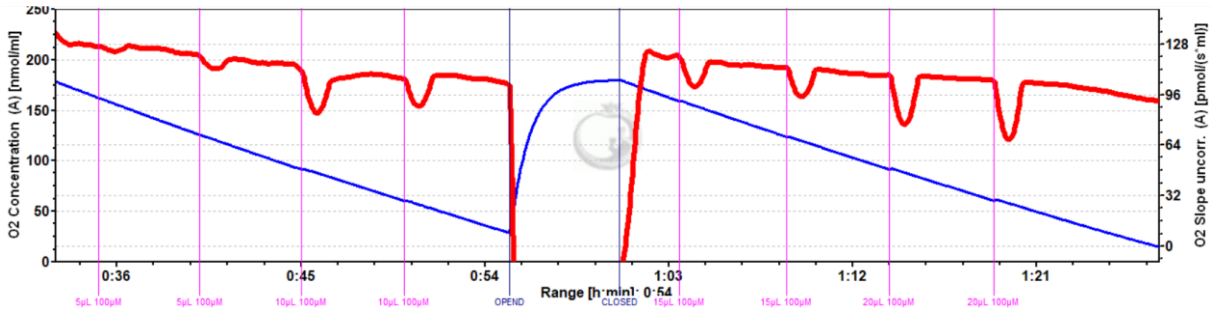
Fig 2.1 Group 1 – MIR experiment I

The blue graph shows continuously measured oxygen concentrations presented (Y-axis to the left, nmol/ml). The red graph shows the time derivative of the oxygen concentrations (Y-axis to the right, as pmol/ (seconds x ml)). This graph displays how oxygen concentration changes in response to addition of MIR06. The time
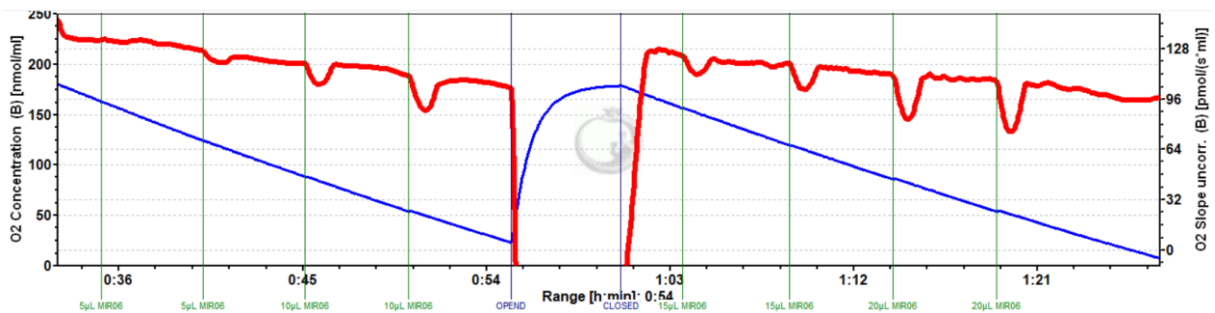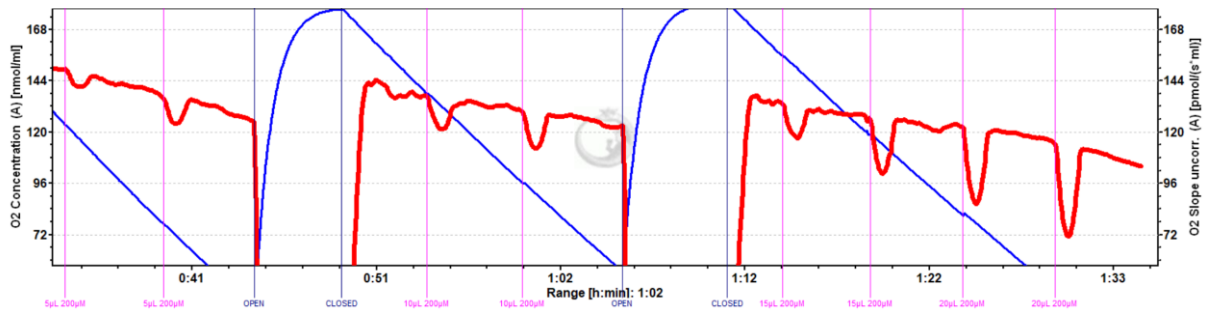
derivative of oxygen consumption is superimposed and displayed as the red graph. Notice the slight dip in the red graph, as was observed in the intervention group. The dips are visible after each successive addition of MIR06. The rapid increase in oxygen concentration is duo to opening of the chambers in order to re-oxygenate them.

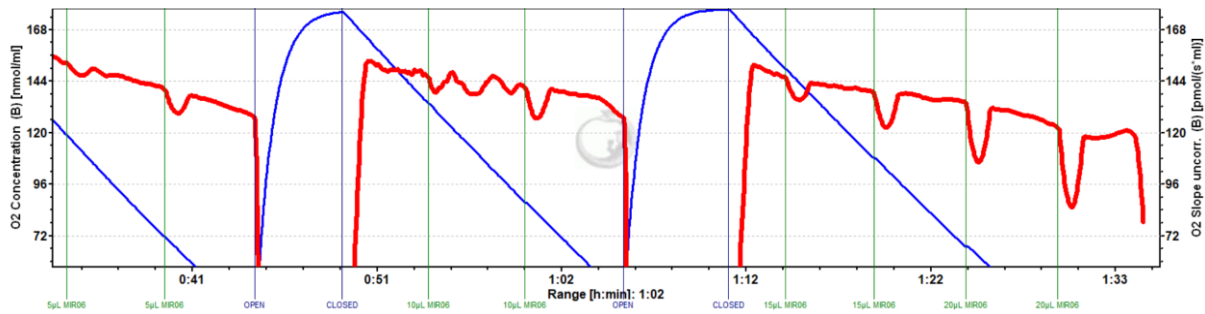## Fig 3.0 Group 3 – 100µM 4-CMC experiment IV

The blue graph shows continuously measured oxygen concentrations presented (Y-axis to the left, nmol/ml). The red graph shows the time derivative of the oxygen concentrations (Y-axis to the right, as pmol/ (seconds x ml)). This graph displays how oxygen concentration changes in response to addition of 100µM 4-CMC. The time derivative of oxygen consumption is superimposed and displayed as the red graph. Notice the slight dip in the red graph after each successive addition of 4-CMC

Fig 3.1 Group 2 – MIR06 experiment IV

The blue graph shows continuously measured oxygen concentrations presented (Y-axis to the left, nmol/ml). The red graph shows the time derivative of the oxygen concentrations (Y-axis to the right, as pmol/ (seconds x ml)). This graph displays how oxygen concentration changes in response to addition of MIR06. The time derivative of oxygen consumption is superimposed and displayed as the red graph. Notice the slight dip in the red graph, as was observed in the intervention group. The dips are visible after each successive addition of MIR06. The rapid increase in oxygen concentration is duo to opening of the chambers in order to re-oxygenate them.

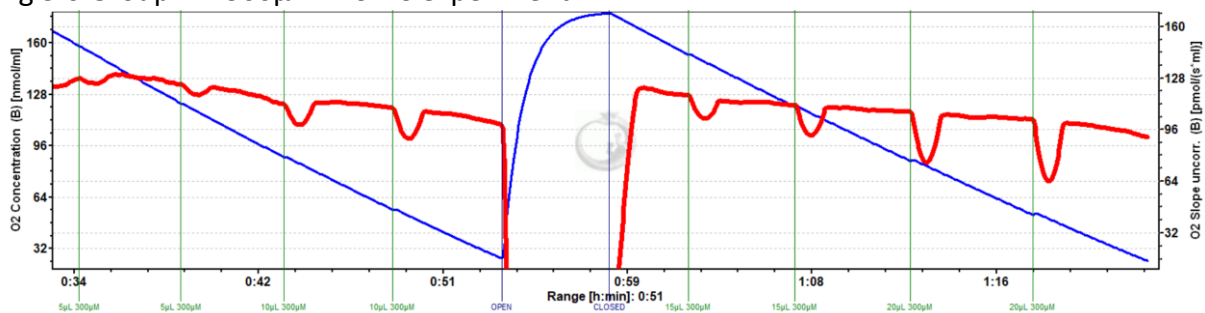## Fig 4.0 Group 3 – 200μM 4-CMC experiment II

The blue graph shows continuously measured oxygen concentrations presented (Y-axis to the left, nmol/ml). The red graph shows the time derivative of the oxygen concentrations (Y-axis to the right, as pmol/ (seconds x ml)). This graph displays how oxygen concentration changes in response to addition of 200μM 4-CMC. The time derivative of oxygen consumption is superimposed and displayed as the red graph. Notice the slight dip in the red graph after each successive addition of 4-CMC. The rapid increase in oxygen concentration is duo to opening of the chambers in order to re-oxygenate them.

Fig 4.1 Group 3 –MIR06 experiment II

The blue graph shows continuously measured oxygen concentrations presented (Y-axis to the left, nmol/ml). The red graph shows the time derivative of the oxygen concentrations (Y-axis to the right, as pmol/ (seconds x ml)). This graph displays how oxygen concentration changes in response to addition of MIR06. The time derivative of oxygen consumption is superimposed and displayed as the red graph. Notice the slight dip in the red graph, as was observed in the intervention group. The dips are visible after each successive addition of MIR06. The rapid increase in oxygen concentration is duo to opening of the chambers in order to re-oxygenate them.
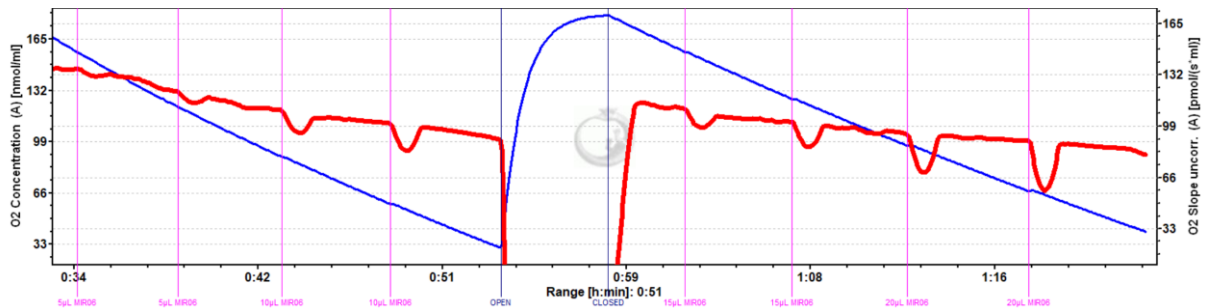
Fig 5.0 Group 4 – 300μM 4-CMC experiment I

The blue graph shows continuously measured oxygen concentrations presented (Y-axis to the left, nmol/ml). The red graph shows the time derivative of the oxygen concentrations (Y-axis to the right, as pmol/ (seconds x ml)). This graph displays how oxygen concentration changes in response to addition of 200μM 4-CMC. The time derivative of oxygen consumption is superimposed and displayed as the red graph. Notice the slight dip in the

red graph after each successive addition of 4-CMC. The rapid increase in oxygen concentration is duo to opening of the chambers in order to re-oxygenate them.

Fig 5.1 Group 4 – MIR06 experiment I

The blue graph shows continuously measured oxygen concentrations presented (Y-axis to the left, nmol/ml). The red graph shows the time derivative of the oxygen concentrations (Y-axis to the right, as pmol/ (seconds x ml)). This graph displays how oxygen concentration changes in response to addition of MIR06. The time derivative of oxygen consumption is superimposed and displayed as the red graph. Notice the slight dip in the red graph, as was observed in the intervention group. The dips are visible after each successive addition of MIR06. The rapid increase in oxygen concentration is duo to opening of the chambers in order to re-oxygenate them.